Epileptogenic networks in drug-resistant epilepsy with amygdala enlargement: Assessment with stereo-EEG and 7 T MRI

Julia Makhalova, Arnaud Le Troter, Sandrine Aubert-Conil, Bernard Giusiano, Aileen Mcgonigal, Agnès Trebuchon, Romain Carron, Samuel Medina Villalon, Christian Bénar, Jean-Philippe Ranjeva, et al.

Epileptogenic networks in drug-resistant epilepsy with amygdala enlargement: Assessment with stereo-EEG and 7T MRI

Julia Makhalova[1,2,3], Arnaud Le Troter[2,3], Sandrine Aubert-Conil[1], Bernard Giusiano[1,4], Aileen McGonigal[1,4], Agnès Trebuchon[1,4], Romain Carron[4,5], Samuel Medina Villalon[1,4], Christian G. Bénar[4], Jean-Philippe Ranjeva[2,3], Maxime Guye[1,2,3], Fabrice Bartolomei[1,4]

[1] APHM, Timone Hospital, Epileptology and Cerebral Rhythmology, Marseille, France

[2] Aix Marseille Univ, CNRS, CRMBM, Marseille, France

[3] APHM, Timone Hospital, CEMEREM, Marseille, France

[4] Aix Marseille Univ, INSERM, INS, Inst Neurosci Syst, Marseille, France

[5] APHM, Timone Hospital, Functional and Stereotactic Neurosurgery, Marseille, France

Corresponding author:

Prof. Fabrice Bartolomei, MD, PhD

Service d'Epileptologie et de Rythmologie cérébrale, Hôpital Timone, 264 Rue Saint-Pierre, 13005, Marseille, France

Tel: +33491385833

Fax: +33491385826

Email: fabrice.bartolomei@ap-hm.fr

Abstract

Objective: Amygdala enlargement is increasingly described in association with temporal lobe epilepsies. Its significance, however, remains uncertain both in terms of etiology and its link with psychiatric disorders and of its involvement in the epileptogenic zone. We assessed the epileptogenic networks underlying drug-resistant epilepsy with amygdala enlargement and investigated correlations between clinical features, epileptogenicity and morphovolumetric amygdala characteristics.

Methods: We identified 12 consecutive patients suffering from drug-resistant epilepsy with visually suspected amygdala enlargement and available stereoelectroencephalographic recording. The epileptogenic zone was defined using the Connectivity Epileptogenicity Index. Morphovolumetric measurements were performed using automatic segmentation and co-registration on the 7TAMIbrain Amygdala atlas.

Results: The epileptogenic zone involved the enlarged amygdala in all but three cases and corresponded to distributed, temporal-insular, temporal-insular-prefrontal or prefrontal-temporal networks in ten cases, while only two were temporo-mesial networks. Morphovolumetrically, amygdala enlargement was bilateral in 75% of patients. Most patients presented psychiatric comorbidities (anxiety, depression, posttraumatic stress disorder). The level of depression defined by screening questionnaire was positively correlated with the extent of amygdala enlargement.

Conclusions: Drug-resistant epilepsy with amygdala enlargement is heterogeneous; most cases implied "temporal plus" networks.

Significance: The enlarged amygdala could reflect an interaction of stress-mediated limbic network alterations and mechanisms of epileptogenesis.

Keywords: amygdala morphometry, Connectivity Epileptogenicity Index, limbic network, pharmacoresistant epilepsy, seizure onset zone, ultra-high-field MRI.

Highlights

- Drug-resistant focal epilepsy with amygdala enlargement is heterogeneous in terms of epileptogenicity.
- Seizure-onset zone involves distributed epileptogenic networks and corresponds to "temporal plus" epilepsies in most cases.
- The extent of amygdala enlargement positively correlated with the level of depression defined by clinical scores.

1 Introduction

Amygdalar enlargement (AE) is a structural abnormality that was first described in temporal lobe epilepsy(Tebartz Van Elst et al., 1999) with normal or non-contributory magnetic resonance imaging (MRI). Along with the development of automated amygdala volumetry techniques since the early 1990s(Amunts et al., 2005)(Bower et al., 2003)(Brierley et al., 2002)(Quattrini et al., 2020), AE has been increasingly reported in patients with different seizure types(Beh et al., 2016)(Coan et al., 2013)(Mitsueda-Ono et al., 2011), as well as in a small proportion of healthy subjects(Reyes et al., 2017). There is now robust evidence for higher prevalence of AE in patients with focal epilepsy as compared to idiopathic generalized epilepsy syndromes and healthy controls(Reyes et al., 2017). A concept linking amygdala enlargement with epileptogenesis has emerged over the last twenty years (Lv et al., 2014)(Takaya et al., 2014)(Suzuki et al., 2019). However, whether there is a specific syndrome associated with AE remains questionable. Furthermore, data on the pathophysiology underlying the enlarged amygdala are sparse (Beh et al., 2016)(Minami et al., 2015). Some authors have suggested an inflammatory process as a putative mechanism leading to the observed amygdala volume and signal changes (Malter et al., 2016)(Na et al., 2020).

At the same time, AE has also been described in several psychiatric entities such as depression and anxiety spectrum disorders that represent common comorbidities with focal drug-resistant epilepsy (Jones et al., 2015)(Suor et al., 2020)(van Eijndhoven et al., 2009). Several studies have outlined the pathogenic role of stress as a causal factor in epileptogenesis (Layne Moore et al., 2009)(Shibahara et al., 2013)(Lanteaume et al., 2009). The existence of correlates of emotional vulnerability in terms of metabolic abnormalities within anterior mesial temporal structures including amygdala, hippocampus and uncus, in patients whose seizures are triggered by emotional events(Lanteaume et al., 2012) suggests the possibility of stress-induced alterations within the affected amygdala. AE in this context could be a hallmark of the

convergence between psychobiological factors (such as stress and/or depression) and epileptogenesis. However, it remains unclear whether the enlarged amygdala should be considered as an authentic epileptogenic lesion analogous to hippocampal sclerosis, or whether it is more likely to be a hub within an altered fronto-temporo-limbic network involved in stress-induced focal seizure genesis. To date, despite a considerable amount of literature on epilepsy with AE, only few cases based on intracerebral electroencephalography (EEG) recordings have been reported (Fan et al., 2020)(Suzuki et al., 2019). Thus, a precise description of epileptogenic network organization has never been performed. Furthermore, accurate assessment of amygdala volume and anatomy is crucial for the diagnosis of AE. Recently, an atlas-based segmentation approach by using multi-contrast magnetic resonance (MR) images and a manual delineation of the amygdala nuclei in a high-resolution MRI group template has been proposed (Tyszka and Pauli, 2016). However, an *in-vivo* amygdala atlas at 7 Tesla that enables morphovolumetry in a single subject, is currently lacking in the literature.

The present study aimed to describe the epileptogenic networks underlying drug-resistant epilepsy with AE and to investigate correlations between clinical features, epileptogenicity and morphovolumetric amygdala characteristics assessed at 7 Tesla.

2 Methods

2.1 Subjects

Across the cohort of 360 patients who underwent stereotactic intracerebral EEG (SEEG) recording presurgical evaluation for drug-resistant focal epilepsy at our center between January 2010 and December 2019, we identified 12 consecutive patients with amygdala enlargement visually suspected on conventional MRI. The presurgical work-up comprised medical history, neurological examination, neuropsychological assessment, ^{18}-fluorodeoxyglucose positron emission tomography (FGD-PET), high-resolution 3Tesla (3T) MRI, long-term scalp-video-

EEG, and subsequent SEEG monitoring. The SEEG exploration was performed as a part of routine clinical management in line with the French national guidelines on stereoelectroencephalography(Isnard et al., 2018). It was indicated in all patients to localize the epileptogenic zone (EZ) and to precisely determine its relations with eloquent areas. Placement of electrodes was selected individually for each patient, based on non-invasive investigations providing hypotheses about the localization of the EZ. All SEEG explorations were bilateral and systematically sampled temporal, insular, frontal, and parietal regions of at least one hemisphere, with ipsilateral pulvinar recordings in eight of 12 cases and contralateral frontal and temporal sampling in all cases.

The French language versions of the Neurological Disorders Depression Inventory-Epilepsy (NDDI-E), with a cutoff score of 15/24, and the 7-item Generalized Anxiety Disorder Scale (GAD-7), with a cutoff score of 7/21, were used for screening for major depressive disorder (MDD) and for generalized anxiety respectively (Gilliam et al., 2006)(Micoulaud-Franchi et al., 2016).

Comparisons of the patient's amygdala volume and morphology were performed against 45 age- and sex-matched healthy subjects without a history of neurological or psychiatric disease.

This study was approved by the local ethics committee (the institutional review board of the Assistance Publique Hopitaux de Marseille, C3BHV2), and informed written consent was obtained for all patients and healthy participants.

2.2 SEEG recordings

SEEG recordings was performed using intracerebral multiple contact electrodes (10–18 contacts with length 2 mm, diameter 0.8 mm, and 1.5 mm apart, Alcis, France) placed under stereotactic conditions using robotized surgical assistant ROSA™. Post-implantation CT scan was routinely used to check the implantation accuracy and exclude intracranial bleeding. Co-

registration of post-implantation CT with pre-implantation MRI and subsequent reconstruction of patient's 3D brain mesh with electrodes were performed using an in-house suite of open-source software tools (EpiTools)(Medina Villalon et al., 2018), to automatically localize the position of each electrode contact and display the results of signal analysis in each patient's anatomy.

Signals were recorded on a Natus system with sampling at 512 Hz or 1024Hz and 16 bits resolution, using a hardware high-pass filter (cut-off at 0.16 Hz at -3 dB) and a hardware anti-aliasing low-pass filter (cut-off at 170Hz or 340Hz, respectively).

2.3 SEEG-signal analysis

All signal analyses were performed in a bipolar montage and computed using the open-source AnyWave software(Colombet et al., 2015) available at https://meg.univ-amu.fr/wiki/AnyWave.

Seizure-onset patterns (SOP) were assessed and defined according to the methodology and electrophysiological criteria established in our previous study(Lagarde et al., 2019). The topographic organization of the epileptogenic network was defined by SEEG-signal analysis. We used a quantified measure called the Connectivity Epileptogenicity Index (cEI) recently developed and validated by our group(Balatskaya et al., 2020). The cEI is a novel approach combining the original Epileptogenicity index (EI) (Bartolomei et al., 2008) and a directed functional connectivity measure ("out-degrees") (Courtens et al., 2016) by non-linear regression coefficient h^2 in a single quantity. Compared to the original epileptogenicity index it has the advantage of being sensitive to all seizure onset modes including those without rapid discharge. "The EI combines analysis of both spectral and temporal features of SEEG signals, respectively, related to the propensity of a brain area to generate fast discharges (12.4– 127 Hz), and to the earliness of involvement of this area in the seizure" (Bartolomei et al., 2017). A normalized EI

value, ranging from 0 (no epileptogenicity) to 1 (maximal epileptogenicity) is used for each considered structure (for detailed methodology see (Bartolomei et al., 2008). The cEI was calculated by using an in house cEI Matlab plugin (https://meg.univ-amu.fr/wiki/AnyWave:Plug-ins). For connectivity analysis, signals were filtered in the beta-gamma range (12–45 Hz). "A nonlinear regression analysis was computed between all pairs of channels based on the h^2 index. The directionality of the link was determined based on the delay of the highest h^2 value across directions. We used a 3 s sliding window with a step of 0.5 s, a maximum lag of 0.1 s. A threshold of 0.2 was applied to the connectivity matrix at each time window, yielding a binary connectivity matrix for each step. The out-degree value for each time window was calculated by computing the number of outgoing connections (out- degrees). The median values of out-degrees were computed across all time windows for each SEEG channel. The normalized values of the h^2 out-degrees and the normalized EI were then summed for each channel. Normalization was performed by dividing all measures by the maximum value of the sum across all channels, resulting in a combined index" (Balatskaya et al., 2020).

In each patient, maximal cEI values from at least three representative seizures were computed and represented within the patient's individual 3D brain map. We labelled SEEG contacts as belonging to the EZ, propagation zone (PZ) or non-involved zone (NIZ), as defined by cEI, based on previous studies(Aubert et al., 2009)(Balatskaya et al., 2020). A cEI value of 0.4 and higher was set as a threshold to define a structure as belonging to the EZ. The PZ was defined as brain areas with $0.1<cEI<0.4$, with sustained discharge during the seizure course. The NIZ was defined as all other brain structures. For statistical analysis at group level, 24 cortical and subcortical brain regions of interest with available SEEG sampling were defined, and all electrode contacts situated within the grey matter were manually assigned to the respective regions.

2.4 MRI acquisition and visual assessment

MRI was performed in all patients and healthy controls (HC) on a 3-Tesla Magnetom Verio MR system (Siemens, Erlangen, Germany) with a 32-channel phased-array head coil and included a 3-dimensional T_1-weighted magnetization-prepared rapid gradient echo (3D-MPRAGE) sequence (TE/TR/TI = 3/2300/900 ms, 160 sections, 256×256 mm² FOV, 256×256 matrix, spatial resolution = (1.0 x 1.0 x 1.0) mm³). Patients also underwent conventional 3T brain MRI acquisitions according to the standardized presurgical epilepsy assessment protocol (axial turbo spin echo (TSE) T_2-weighted (T_2-w), axial gradient echo (GE) T_2-w, 3D-fluid-attenuated inversion recovery (FLAIR), 3D-inversion recovery (IR), and post-gadolinium 3D-T_1-weighted (T_1-w) images).

Additionally, ultra-high-field MR images were acquired in 6 out of 12 patients and in all healthy controls on a 7Tesla (7T) Magnetom MR system (Siemens, Erlangen, Germany) using a 32-channel (32Rx/1Tx) head coil. The protocol included a 3-dimensional T_1-weighted magnetization-prepared 2 rapid acquisition gradient echoes sequence (T_1-w MP2RAGE, TR = 5000 ms/TE = 3 ms/TI1 = 900 ms/TI2 = 2750 ms, 256 slices, spatial resolution = (0.6 x 0.6 x 0.6) mm^3, acquisition time = 10 min).

Conventional MRI was interpreted by experienced neuroradiologists and also independently assessed by three neurologists (F.B., S.A. and J.S.). The visual diagnosis of a suspected AE was made if concordance was reached among the three investigators.

In patients with available 7T acquisitions, the amygdala anatomy has been assessed visually (F.B., J.S.) both on 3T MPRAGE and on 7T MP2RAGE images.

2.5 Amygdala segmentation and morphovolumetric analysis

A fully automatic morphovolumetric analysis of the amygdala was performed in all patients and HC (Fig 1). It comprised automated volumetric segmentation obtained by non-linear

registration using an in house high-resolution 7T MRI template targeted at 0.5 mm3, 7TAMIBrain (Besson et al., 2016) and applied on a corresponding Amygdala atlas, manually delineated. Manual segmentation of the amygdala region (Fig 1A) was performed by an expert in the 7TAMIBrain space, bilaterally, on each slice in the three planes (first pass on axial views, regularized on second and third pass in the sagittal and coronal views). An atlas-based automatic segmentation of the amygdala (Fig 1B) in the subject space was performed using a symmetric diffeomorphic image registration process, with default parameters for a symmetric image normalization (SyN) transformation model. Finally, for each patient (3T or 7T) and healthy control (7T), all 3D morphometric measures (Fig 1C) were directly extracted in the subject spaces from this segmentation mask of the left and right amygdala (Fig 1B), warped to the individual subject's anatomy(Avants et al., 2008). Left and right amygdala volumes, elongation and eccentricity metrics were computed(Avants et al., 2014). The elongation was defined as the ratio between the lengths of the principal axis (MajorAxisLength) and a secondary axis (MinorAxisLength), defined by the equivalent ellipsoid obtained after applying principal component analysis. The eccentricity was defined as $\sqrt{(MajorAxisLength^2 - MinorAxisLength^2)}/MajorAxisLength$. Eccentricity near 0 corresponds to a circular shape whereas eccentricity near 1 refers to a shape approaching a line. The volume (in mm^3) is the number of voxels in the region of interest (ROI), multiplied by the image resolution.

Left and right amygdala volumes were normalized by total intracranial volume extraction (using the Brain Extraction Tool (BET) command from FSL FMRIB (Functional MRI of the Brain) Software Library v6.0(Jenkinson et al., 2012)) to control for individual differences in brain size. BET was applied directly to the T_1-w images at 3T, and to the INV2 images from MP2RAGE at 7T. Volume asymmetry was defined as the absolute volume difference divided by the sum of the compared volumes.

2.6 Statistical analysis

Statistical analyses were performed using JMP9 (SAS Institute). Z-scores of normalized amygdala volumes were computed for the right and left amygdala of each patient relative to mean values of the right and the left amygdala in HC respectively (z-score = (patient's individual amygdala volume – HC group amygdala volume mean)/HC group amygdala volume standard deviation). In the same way, z-scores of morphometric measures (eccentricity and elongation) for each patient's right and left amygdala were computed. Amygdala enlargement was defined as increase of the normalized amygdala volume and/or increase of amygdala eccentricity or elongation with a z-score more than 2 standard deviations above the HC mean. A normalized amygdala volume increase with z-score between 1.5 and 2.0 was defined as borderline AE (Coan et al., 2013). Amygdala volume asymmetry more than 6% (z-score >2.0) was considered as significant.

For group level analyses, normal distribution was assessed visually and by using the Kolmogorov–Smirnov test. The amygdala volumes of patients and HC were normally distributed. Independent sample two-tailed t test was used to assess group differences in amygdala volume, eccentricity, or elongation between the patients' epileptogenic amygdala (belonging to the EZ or PZ as defined by SEEG quantitative analysis) and patients' non-involved amygdala. The Spearman rank-order correlation coefficient was used to compute correlations between the patients' amygdala volume, eccentricity, or elongation and the amygdala epileptogenicity values (as defined by the cEI), and between the patients' enlarged amygdala volume and clinical variables (mean seizure frequency, age at onset, duration of epilepsy, NDDI-E and GAD-7 scores), or a number of brain regions involved in the EZ or the PZ network, respectively. In cases with volumetrically bilateral amygdala enlargement the patient's maximal amygdala volume was used.

A p-value <0.05 was considered as significant.

3 Results

3.1 Clinical features

Patients' clinical characteristics are summarized in Table 1. Mean age at epilepsy onset was 20.6 years (range 4-42), mean duration of epilepsy was 15 years (range 3-33). Eight of 12 patients (75%) presented generalized anxiety disorder (n=3), depression (n=3), post-traumatic stress disorder (PTSD, n=1), or bipolar disorder (n=1) prior to epilepsy onset. At time of evaluation, 8/12 patients (66.7%) fulfilled screening diagnostic criteria for high probability of major depression (NDDI-E ≥ 15), and 10/12 (83.3%) fulfilled screening diagnostic criteria for high probability of generalized anxiety disorder (GAD-7 ≥7). Psychotraumatic events occurring prior to epilepsy onset were documented in five (42%) patients. Mean seizure frequency was 12 per month (range 2-30). Various subjective initial ictal signs (auras) were observed, and comprised lateralized painful tingling, heat or burning sensation (50%), ascending epigastric sensation (25%), dizziness or floating (25%), anxiety or intense fear (25%), auditory illusions (16.7%), euphoric or well-being sensation (16.7%), déjà-vu (16.7%) or unpleasant anticipatory sensation (8.3%). Objective semiology as observed on video-EEG included patterns suggestive of temporal lobe seizures (behavioral arrest, oro-alimentary, verbal and/or gestural automatisms, uni- or bilateral dystonic hand posture, altered awareness), or more complex features suggestive of insulo-perisylvian or frontal involvement (facial contraction, salivation and/or other autonomic signs, head version, bilateral tonic phenomena or psychomotor agitation). All patients had alteration of consciousness during their seizures. Some also experienced isolated auras. Bilateral tonic-clonic seizures were absent or rare in 75% of patients.

A unilateral AE was suspected on MRI by visual analysis. It was an isolated finding in eight patients, was associated with the presence of increased signal on FLAIR of the enlarged

amygdala in four cases, and with ipsilateral increased FLAIR signal in the temporo-polar region in one case.

Nine of 12 patients underwent resective surgery following SEEG exploration. The remaining three were recused because of the bilateral epileptogenic zone in two and of a high risk of post-surgical functional deficit in one. The post-surgical outcome was favorable in four (Engel class I and II, 44.4%), with worthwhile improvement in four (Engel class III, 44.4%), and without significant improvement in one case (Engel class IV, 11.2%). Histopathological abnormalities were detected in the neocortex and/or the hippocampus: focal cortical dysplasia (FCD) in five patients (type1 n=3, type2b n=1, type3a n=1), mild gliosis in two patients, and hippocampal sclerosis in two patients. Noteworthy, histopathology of the amygdala was not available due to the surgical technique (aspiration), except for the case with FCD2b affecting the amygdala and the temporal pole.

3.2 Organization of the epileptogenic network

Seizure-onset patterns (SOP) involved low-voltage fast activity (LVFA) in two (16.7%) cases, while ten (83.3%) cases were characterized by seizure initiation at lower frequencies (<14.4Hz). The prevalence of different SOP types was, in decreasing order: theta-alpha sharp waves (41.7%), beta sharp waves (25%), slow wave /Direct Current (DC) shift followed by LVFA (16.7%), delta-brush (8.3%) and rhythmic spikes /spike-waves (8.3%).

The EZ defined by visual analysis and cEI quantification included the enlarged amygdala in all but three cases, in which it was a part of the PZ. The epileptogenic network (brain regions within the EZ and the PZ), was always complex, systematically involving both temporal and extratemporal structures, including mesial temporal, lateral temporal, insular, dorso-lateral and ventro-lateral prefrontal, orbito-frontal cortex, and pulvinar, with bilateral implication in 83.3% of cases. The premotor and primary motor cortices as well as parietal regions were rarely involved. Interestingly, of the two subcortical structures sampled in this series, the pulvinar

thalami (n=8) and the head of the caudate nucleus (n=4), only the former was implicated during seizures.

Epileptogenicity profiles across different brain regions at group level are shown in Fig 2. The enlarged amygdala exhibited the highest mean cEI values followed by ipsilateral hippocampus, rhinal cortex, anterior temporal lateral and ventrolateral prefrontal regions, all with cEI > 0.4. The posterior temporal, posterior insular regions and thalamus showed moderate epileptogenicity values (0.4>cEI>0.3), the anterior insula, the remaining prefrontal, motor-premotor and inferior parietal regions were less epileptogenic (0.3>cEI>0.2), whereas the primary sensory cortex and the superior parietal lobule showed very low epileptogenicity values (cEI<0.2) when involved (Fig 2A). and exhibited moderate to high cEI values in all but one case. Four distinct profiles of epileptogenic network organization were identified according to the spatial distribution of the main epileptogenic regions (cEI>0.4): mesial temporal (n=2), temporo-insular (n=6), temporo-insular-prefrontal (n=2), and prefrontal-temporal mesial (n=2) (Fig 2B).

An illustrative case of focal epilepsy with AE and the lateral temporo-insular epileptogenic network involving the enlarged amygdala is shown in Fig 3.

3.3 Amygdala morphovolumetric characteristics

The amygdala morphometric and volumetric features at individual patient level are summarized in Table 2. The presence of visually suspected AE was quantitatively confirmed in all patients (n=12), based on the above-defined combined morphovolumetric criteria. Volumetrically, significant AE (z-scores >2.0) was detected in nine out of twelve patients (75%). Considered as unilateral by visual analysis, it proved to be bilateral at quantitative assessment. Unilateral borderline AE (1.5<z-scores <2.0) was detected in three remaining patients. A significant amygdala volume asymmetry (> 6%) was found in three patients.

Morphometric analysis showed significant increase in eccentricity of the amygdala compared to controls in five patients (two with a volumetrically significant AE and three with a borderline AE). Significant increase in amygdala elongation was demonstrated in three patients (two with a volumetrically significant, and one with a borderline AE). These morphometric changes, indicating a more elongated shape of the amygdala (eccentricity) or an increased length along its major axis (elongation), were bilateral when present.

We examined the correlations between the morphovolumetric and clinical features. We found a significant positive correlation between the patient's enlarged amygdala volumes and the NDDI-E scores ($p=0.04$, $r=0.582$). There was no statistically significant correlation between the amygdala volume and age at epilepsy onset, epilepsy duration, seizure frequency, or GAD-7 scores, nor between the amygdala eccentricity or elongation and any of the assessed clinical variables.

We then looked for a correlation between the morphovolumetric characteristics and epileptogenicity. There was no statistically significant correlation between the amygdala volume and cEI values, nor between the morphometric parameters (eccentricity, elongation) and cEI values. Furthermore, there was no statistically significant difference in amygdala volume, eccentricity, or elongation between the patients' epileptogenic amygdala (belonging to the EZ or PZ) and patients' non-involved amygdala. By the same way, we found no correlation between the amygdala volume and the number of brain regions involved in the EZ ($p=0.79$) or the PZ network ($p=0.34$).

3.4 Amygdala anatomy by visual assessment

Major amygdala nuclei and nuclear groups (lateral, basolateral, basomedial, central and cortico-medial) could be distinguished by visual inspection on MP2RAGE Uni-Den images in patients with available 7T MRI. The visually detectable asymmetry between the right and the left amygdala was observed on these images, offering better spatial resolution compared to 3T, as

an extension of the lateral nucleus dorso-laterally towards the neighboring claustrum, as well as of the central nucleus laterally towards the temporal limb of the anterior commissure, within the amygdalo-striatal transition area (Fig 3B).

4 Discussion

The present study is the first to provide a quantified assessment of epileptogenic networks underlying drug-resistant focal epilepsy with AE while searching for possible links between clinical features, electrophysiological epileptogenicity patterns and quantitative amygdala measurements at 7T.

AE has been described in patients with "negative" MRI and proposed to be a new epileptic syndrome by some authors. A recent review reported that patients with AE could present with late onset, focal seizures and good therapeutic response in the majority of cases (80%)(Beh et al., 2016). In the present series we focused on patients with drug-resistant epilepsy associated with AE who underwent SEEG. Mean age at epilepsy onset (20.6 y) was younger than reported in the literature for patients with epilepsy and AE (32 y)(Beh et al., 2016)(Suzuki et al., 2019), while mean seizure frequency and epilepsy duration did not differ from previous series. Interestingly, subjective semiology was dominated by lateralized unpleasant or painful sensations of different modalities (sensory, somatosensory, autonomic).

4.1 Epileptogenic network organization

Some previous studies considered focal epilepsy with AE as a subtype of mesial temporal lobe epilepsy (Fan et al., 2020)(Lv et al., 2014)(Suzuki et al., 2019). Our data demonstrated that the enlarged amygdala was integrated in more complex epileptogenic networks, which in most cases largely extended beyond the mesial temporal region. The amygdala was one of the core epileptogenic structures within the distributed epileptogenic network that preferentially involved temporal (mesial, lateral, or both), insular, ventro-lateral prefrontal, ventro-mesial

prefrontal regions and pulvinar. Based on the Connectivity Epileptogenicity index(Balatskaya et al., 2020), we could identify four distinct patterns of epileptogenic network organization, with the temporo-insular type being the most common, encountered in half of cases, followed by equally represented temporo-insular-prefrontal, prefrontal-temporal mesial, and mesial temporal types. It is likely that our selection of drug-resistant cases with SEEG induced a bias in the selection of more complex cases. However, unlike two previously published series of invasively explored temporal epilepsy with AE(Fan et al., 2020)(Suzuki et al., 2019) having the same selection bias, pure mesial temporal organization of the EZ was present in only a small proportion of patients (12.5%). In three cases, the enlarged amygdala was not a part of the epileptogenic zone, and in the whole cohort we did not find correlation between the amygdala volumes and the extension of the epileptogenic zone network, nor between the amygdala volume and epileptogenicity values. Therefore, we can consider that the enlarged amygdala does not appear to be a specific epileptogenic lesion, but it is rather a marker of distributed epileptogenic networks.

Furthermore, we found high epileptogenicity values within the ipsilateral pulvinar and a high proportion of cases with bilateral involvement. These factors might have contributed to a less favorable surgical outcome in the present series (22.2% seizure-free) which is in contrast to an excellent surgical prognosis (more than 80% seizure-free) in the above-mentioned series and which is poorer than reported in MRI-negative temporal epilepsy (seizure-free rates varying from 36 to 76%)(Mariani et al., 2019) or as compared to general surgical results following SEEG exploration (59-64% seizure-free)(Cardinale et al., 2019)(Trebuchon et al., 2021).

4.2 Amygdala morphovolumetric features

In the present study, the amygdala morphovolumetric features were assessed by using an original approach combining automatic atlas-based segmentation of amygdala, with co-registration on the 7T AMIBrain Amygdala atlas. It allows good detection of moderate

amygdala volume changes and estimation of morphometric features at individual subject level. We could demonstrate that significant increase in normalized amygdala volume compared to HC was present bilaterally in 75% of patients, despite a unilateral AE initially suspected by visual analysis, with the largest amygdala being situated contralaterally to the EZ in 42%. The observed discrepancies between the volumetric findings and visual diagnosis indicate that the perceived asymmetry reflects the amygdala shape modification rather than a total, mostly bilateral volume increase. This visually distinguishable shape modification is likely due to the extension of the lateral and central amygdala nuclei dorso-laterally, towards the neighboring claustrum and striatum. The physiological connectivity patterns of the respective nuclei fit well with this hypothesis. The lateral nucleus represents the principal entry point of the amygdala, receiving inputs from cortical sensory systems, hippocampus and thalamus, and the central nucleus is a key output region for emotional processing and associated physiological responses, in particular for autonomic and somatic signs of fear and anxiety(Davis and Whalen, 2001)(Sah et al., 2003). However, whether the distinct types of epileptogenic networks associated with AE would preferentially involve some particular amygdala nuclei remains to be investigated.

4.3 Link with psychiatric comorbidities

It has been suggested that AE could be related to psychiatric comorbidities(Tebartz Van Elst et al., 2002)(Lv et al., 2014). This hypothesis is appealing, but such a link has not been found in all studies. In our series, we observed a high prevalence of depression and anxiety symptoms (66.7% and 83.3.% respectively, as defined by the clinical screening scores). This is much higher than the pooled prevalence of these comorbidities reported in a meta-analysis, which showed prevalence of depressive disorders in people with epilepsy to be 20.2% and anxiety disorders 22.9%, across studies using Diagnostic and Statistical Manual of Mental Disorders (DSM) criteria(Scott et al., 2017). While screening tools cannot be considered equivalent to psychiatric diagnosis, it is of interest that in our series, the level of depression defined by clinical

scores (NDDI-E) significantly correlated with the extent of AE, possibly suggesting a link between these two conditions in our patients. AE could also be related to stress and traumatic life events. Indeed, in mature animals, major social stress may lead to depression, increased amygdala volume and susceptibility to epileptogenesis(Becker et al., 2015). In humans, traumatic life events could be risk factors for developing epilepsy(Gélisse et al., 2015)(Lanteaume et al., 2012)(Shibahara et al., 2013). A psychotraumatic or stressful event has been identified in as many as 42% of our patients, prior to onset of their epilepsy. In the light of our data, the hypothesis of a causal or aggravating role of stress factors is plausible. Such a "double-hit" mechanism could promote the development of epileptogenesis in patients with pre-existing lesions. A focal cortical dysplasia was found in half of our cases; a subsequent stressful event could potentially act as a "second hit" in already vulnerable patients and trigger epileptogenesis(Bernard, 2016).

4.4 Limitations of the study

Some limitations of this study are important to be mentioned. First, focusing on the SEEG-explored patients represents a selection bias towards more complex cases, with additional limitation due to the sampling problem: while offering an advantage of a three-dimensional probing of epileptogenic networks, SEEG-derived electrophysiological data provide the information limited to the recorded brain areas. Thus, an incomplete sampling of the EZ remains possible, in particular in patients with unfavorable surgical outcome. However, extensive, bilateral explorations were performed in all our cases. Further limitation is the small sample size of our cohort that might reflect a low prevalence of drug-resistant focal epilepsy with AE, given the high drug-responder rates reported in the literature(Na et al., 2020). Finally, the present study did not compare amygdala connectivity or epileptogenic network profiles between AE patients and a control group of patients with normal amygdala size, which could be a subject of future research in a larger patient population.

In conclusion, drug-resistant epilepsy with morphovolumetrically confirmed uni- or bilateral amygdala enlargement is heterogeneous in terms of epileptogenicity. In the majority of cases, "temporal plus" or "perisylvian" epilepsies(Barba et al., 2007)(Bartolomei et al., 2010) were observed. The enlarged amygdala is one of the core epileptogenic structures within distributed epileptogenic networks, however its links with epileptogenicity appear complex. Finally, observed correlation between degree of amygdala enlargement and NNDI-E scores at the individual patient level reinforces the hypothesis that the enlarged amygdala could represent a key radiological sign of a stress-mediated limbic network disease associating focal epilepsy and depression as clinical features.

Acknowledgements

This work was performed by a laboratory member of France Life Imaging network (grant ANR-11-INBS-0006) on the platform 7T-AMI, supported by a French “Investissements d’Avenir” program (grant ANR-11-EQPX-0001) and by Excellence Initiative of Aix-Marseille University, A*MIDEX.

Declaration of interest

None of the authors have potential conflicts of interest to be disclosed.

References

Amunts K, Kedo O, Kindler M, Pieperhoff P, Mohlberg H, Shah NJ, et al. Cytoarchitectonic mapping of the human amygdala, hippocampal region and entorhinal cortex: Intersubject variability and probability maps. Anat. Embryol. (Berl)., vol. 210, Anat Embryol (Berl); 2005, p. 343–52. https://doi.org/10.1007/s00429-005-0025-5.

Aubert S, Wendling F, Regis J, McGonigal A, Figarella-Branger D, Peragut JC, et al. Local and remote epileptogenicity in focal cortical dysplasias and neurodevelopmental tumours. Brain 2009;132:3072–86. https://doi.org/10.1093/brain/awp242.

Avants BB, Epstein CL, Grossman M, Gee JC. Symmetric diffeomorphic image registration with cross-correlation: Evaluating automated labeling of elderly and neurodegenerative brain. Med Image Anal 2008;12:26–41. https://doi.org/10.1016/j.media.2007.06.004.

Avants BB, Tustison NJ, Stauffer M, Song G, Wu B, Gee JC. The Insight ToolKit image registration framework. Front Neuroinform 2014;8. https://doi.org/10.3389/fninf.2014.00044.

Balatskaya A, Roehri N, Lagarde S, Pizzo F, Medina S, Wendling F, et al. The "Connectivity Epileptogenicity Index " (cEI), a method for mapping the different seizure onset patterns in StereoElectroEncephalography recorded seizures. Clin Neurophysiol 2020;131:1947–55. https://doi.org/10.1016/j.clinph.2020.05.029.

Barba C, Barbati G, Minotti L, Hoffmann D, Kahane P. Ictal clinical and scalp-EEG findings differentiating temporal lobe epilepsies from temporal "plus" epilepsies. Brain 2007;130:1957–67. https://doi.org/10.1093/brain/awm108.

Bartolomei F, Chauvel P, Wendling F. Epileptogenicity of brain structures in human temporal lobe epilepsy: A quantified study from intracerebral EEG. Brain 2008. https://doi.org/10.1093/brain/awn111.

Bartolomei F, Cosandier-Rimele D, McGonigal A, Aubert S, Régis J, Gavaret M, et al. From mesial temporal lobe to temporoperisylvian seizures: A quantified study of temporal lobe seizure networks. Epilepsia 2010;51:2147–58. https://doi.org/10.1111/j.1528-1167.2010.02690.x.

Bartolomei F, Lagarde S, Wendling F, McGonigal A, Jirsa V, Guye M, et al. Defining epileptogenic networks: Contribution of SEEG and signal analysis. Epilepsia 2017;58:1131–47. https://doi.org/10.1111/epi.13791.

Becker C, Bouvier E, Ghestem A, Siyoucef S, Claverie D, Camus F, et al. Predicting and treating stress-Induced vulnerability to epilepsy and depression. Ann Neurol 2015;78:128–36. https://doi.org/10.1002/ana.24414.

Beh SMJ, Cook MJ, D'Souza WJ. Isolated amygdala enlargement in temporal lobe epilepsy: A systematic review. Epilepsy Behav 2016;60:33–41. https://doi.org/10.1016/j.yebeh.2016.04.015.

Bernard C. The diathesis-epilepsy model: How past events impact the development of epilepsy and comorbidities. Cold Spring Harb Perspect Med 2016;6. https://doi.org/10.1101/cshperspect.a022418.

Besson P, LeTroteur A, Sein J, Brun G, Guye M, Ranjeva JP. 7TAMIbrainT1w_30 : Whole-brain ultra-high resolution average T1-weighted template at 7 Tesla to improve in vivo depiction of small brain structures. 24th ISMRM Annu. Meet. Exhib. 2016 25th SMRT Annu. Meet. 2016, Singapore: Curran Associates, Inc. 57 Morehouse Lane Red Hook, NY 12571 USA; 2016, p. 6801. ISBN: 978-1-5108-3768-3.

Bower SPC, Vogrin SJ, Morris K, Cox I, Murphy M, Kilpatrick CJ, et al. Amygdala volumetry in "imaging-negative" temporal lobe epilepsy. J Neurol Neurosurg Psychiatry 2003;74:1245–9. https://doi.org/10.1136/jnnp.74.9.1245.

Brierley B, Shaw P, David AS. The human amygdala: A systematic review and meta-analysis of volumetric magnetic resonance imaging. Brain Res Rev 2002;39:84–105. https://doi.org/10.1016/S0165-0173(02)00160-1.

Cardinale F, Rizzi M, Vignati E, Cossu M, Castana L, D'Orio P, et al. Stereoelectroencephalography: Retrospective analysis of 742 procedures in a single centre. Brain 2019;142:2688–704. https://doi.org/10.1093/brain/awz196.

Coan AC, Morita ME, de Campos BM, Yasuda CL, Cendes F. Amygdala Enlargement in Patients with Mesial Temporal Lobe Epilepsy without Hippocampal Sclerosis. Front Neurol 2013;4. https://doi.org/10.3389/fneur.2013.00166.

Colombet B, Woodman M, Badier JM, Bénar CG. AnyWave: A cross-platform and modular software for visualizing and processing electrophysiological signals. J Neurosci Methods 2015. https://doi.org/10.1016/j.jneumeth.2015.01.017.

Courtens S, Colombet B, Trébuchon A, Brovelli A, Bartolomei F, Bénar CG. Graph Measures of Node Strength for Characterizing Preictal Synchrony in Partial Epilepsy. Brain Connect

2016;6:530–9. https://doi.org/10.1089/brain.2015.0397.

Davis M, Whalen PJ. The amygdala: vigilance and emotion. vol. 6. 2001.

van Eijndhoven P, van Wingen G, van Oijen K, Rijpkema M, Goraj B, Jan Verkes R, et al. Amygdala Volume Marks the Acute State in the Early Course of Depression. Biol Psychiatry 2009;65:812–8. https://doi.org/10.1016/j.biopsych.2008.10.027.

Fan Z, Sun B, Lang L qin, Hu J, Hameed NUF, Wei Z xuan, et al. Diagnosis and surgical treatment of non-lesional temporal lobe epilepsy with unilateral amygdala enlargement. Neurol Sci 2020. https://doi.org/10.1007/s10072-020-04794-8.

Gélisse P, Genton P, Coubes P, Tang NPL, Crespel A. Can emotional stress trigger the onset of epilepsy? Epilepsy Behav 2015;48:15–20. https://doi.org/10.1016/j.yebeh.2015.05.010.

Gilliam FG, Barry JJ, Hermann BP, Meador KJ, Vahle V, Kanner AM. Rapid detection of major depression in epilepsy: a multicentre study. Lancet Neurol 2006;5:399–405. https://doi.org/10.1016/S1474-4422(06)70415-X.

Isnard J, Taussig D, Bartolomei F, Bourdillon P, Catenoix H, Chassoux F, et al. French guidelines on stereoelectroencephalography (SEEG). Neurophysiol Clin 2018;48:5–13. https://doi.org/10.1016/j.neucli.2017.11.005.

Jenkinson M, Beckmann CF, Behrens TEJ, Woolrich MW, Smith SM. FSL. Neuroimage 2012;62:782–90. https://doi.org/10.1016/j.neuroimage.2011.09.015.

Jones JE, Jackson DC, Chambers KL, Dabbs K, Hsu DA, Stafstrom CE, et al. Children with epilepsy and anxiety: Subcortical and cortical differences. Epilepsia 2015;56:283–90. https://doi.org/10.1111/epi.12832.

Lagarde S, Buzori S, Trebuchon A, Carron R, Scavarda D, Milh M, et al. The repertoire of seizure onset patterns in human focal epilepsies: Determinants and prognostic values. Epilepsia 2019;60:85–95. https://doi.org/10.1111/epi.14604.

Lanteaume L, Bartolomei F, Bastien-Toniazzo M. How do cognition, emotion, and epileptogenesis meet? A study of emotional cognitive bias in temporal lobe epilepsy. Epilepsy Behav 2009;15:218–24. https://doi.org/10.1016/j.yebeh.2009.03.034.

Lanteaume L, Guedj E, Bastien-Toniazzo M, Magalahaes A, Mundler O, Bartolomei F. Cognitive and metabolic correlates of emotional vulnerability in patients with temporal lobe epilepsy. J Neurol Neurosurg Psychiatry 2012;83:522–8. https://doi.org/10.1136/jnnp-2011-

301219.

Layne Moore J, Elliott JO, Lu B, Klatte ET, Charyton C. Serious psychological distress among persons with epilepsy based on the 2005 California Health Interview Survey. Epilepsia 2009;50:1077–84. https://doi.org/10.1111/j.1528-1167.2008.01996.x.

Lv RJ, Sun ZR, Cui T, Guan HZ, Ren HT, Shao XQ. Temporal lobe epilepsy with amygdala enlargement: A subtype of temporal lobe epilepsy. BMC Neurol 2014;14. https://doi.org/10.1186/s12883-014-0194-z.

Malter MP, Widman G, Galldiks N, Stoecker W, Helmstaedter C, Elger CE, et al. Suspected new-onset autoimmune temporal lobe epilepsy with amygdala enlargement. Epilepsia 2016;57:1485–94. https://doi.org/10.1111/epi.13471.

Mariani V, Revay M, D'Orio P, Rizzi M, Pelliccia V, Nichelatti M, et al. Prognostic factors of postoperative seizure outcome in patients with temporal lobe epilepsy and normal magnetic resonance imaging. J Neurol 2019;266:2144–56. https://doi.org/10.1007/s00415-019-09394-x.

Medina Villalon S, Paz R, Roehri N, Lagarde S, Pizzo F, Colombet B, et al. EpiTools, A software suite for presurgical brain mapping in epilepsy: Intracerebral EEG. J Neurosci Methods 2018;303:7–15. https://doi.org/10.1016/j.jneumeth.2018.03.018.

Micoulaud-Franchi JA, Lagarde S, Barkate G, Dufournet B, Besancon C, Trébuchon-Da Fonseca A, et al. Rapid detection of generalized anxiety disorder and major depression in epilepsy: Validation of the GAD-7 as a complementary tool to the NDDI-E in a French sample. Epilepsy Behav 2016;57:211–6. https://doi.org/10.1016/j.yebeh.2016.02.015.

Minami N, Morino M, Uda T, Komori T, Nakata Y, Arai N, et al. Surgery for amygdala enlargement with mesial temporal lobe epilepsy: Pathological findings and seizure outcome. J Neurol Neurosurg Psychiatry 2015;86:887–94. https://doi.org/10.1136/jnnp-2014-308383.

Mitsueda-Ono T, Ikeda A, Inouchi M, Takaya S, Matsumoto R, Hanakawa T, et al. Amygdalar enlargement in patients with temporal lobe epilepsy. J Neurol Neurosurg Psychiatry 2011;82:652–7. https://doi.org/10.1136/jnnp.2010.206342.

Na HK, Lee HJ, Hong SJ, Lee DH, Kim KM, Lee HW, et al. Volume change in amygdala enlargement as a prognostic factor in patients with temporal lobe epilepsy: A longitudinal study. Epilepsia 2020;61:70–80. https://doi.org/10.1111/epi.16400.

Quattrini G, Pievani M, Jovicich J, Aiello M, Bargalló N, Barkhof F, et al. Amygdalar nuclei

and hippocampal subfields on MRI: Test-retest reliability of automated volumetry across different MRI sites and vendors. Neuroimage 2020;218. https://doi.org/10.1016/j.neuroimage.2020.116932.

Reyes A, Thesen T, Kuzniecky R, Devinsky O, McDonald CR, Jackson GD, et al. Amygdala enlargement: Temporal lobe epilepsy subtype or nonspecific finding? Epilepsy Res 2017;132:34–40. https://doi.org/10.1016/j.eplepsyres.2017.02.019.

Sah P, Faber ESL, De Armentia ML, Power J. The amygdaloid complex: Anatomy and physiology. Physiol Rev 2003;83:803–34. https://doi.org/10.1152/physrev.00002.2003.

Scott AJ, Sharpe L, Hunt C, Gandy M. Anxiety and depressive disorders in people with epilepsy: A meta-analysis. Epilepsia 2017;58:973–82. https://doi.org/10.1111/epi.13769.

Shibahara I, Osawa SI, Kon H, Morita T, Nakasato N, Tominaga T, et al. Increase in the number of patients with seizures following the Great East-Japan Earthquake. Epilepsia 2013;54. https://doi.org/10.1111/epi.12070.

Suor JH, Jimmy J, Monk CS, Phan KL, Burkhouse KL. Parsing differences in amygdala volume among individuals with and without social and generalized anxiety disorders across the lifespan. J Psychiatr Res 2020;128:83–9. https://doi.org/10.1016/j.jpsychires.2020.05.027.

Suzuki H, Sugano H, Nakajima M, Higo T, Iimura Y, Mitsuhashi T, et al. The epileptogenic zone in pharmaco-resistant temporal lobe epilepsy with amygdala enlargement. Epileptic Disord 2019;21:252–64. https://doi.org/10.1684/epd.2019.1075.

Takaya S, Ikeda A, Mitsueda-Ono T, Matsumoto R, Inouchi M, Namiki C, et al. Temporal Lobe Epilepsy with Amygdala Enlargement: A Morphologic and Functional Study. J Neuroimaging 2014;24:54–62. https://doi.org/10.1111/j.1552-6569.2011.00694.x.

Tebartz Van Elst L, Baeumer D, Lemieux L, Woermann FG, Koepp M, Krishnamoorthy S, et al. Amygdala pathology in psychosis of epilepsy: A magnetic resonance imaging study in patients with temporal lobe epilepsy. Brain 2002;125:140–9. https://doi.org/10.1093/brain/awf008.

Tebartz Van Elst L, Woermann FG, Lemieux L, Trimble MR. Amygdala enlargement in dysthymia - A volumetric study of patients with temporal lobe epilepsy. Biol Psychiatry 1999;46:1614–23. https://doi.org/10.1016/S0006-3223(99)00212-7.

Trebuchon A, Racila R, Cardinale F, Lagarde S, McGonigal A, Lo Russo G, et al. Electrical stimulation for seizure induction during SEEG exploration: A useful predictor of

postoperative seizure recurrence? J Neurol Neurosurg Psychiatry 2021;92:22–6. https://doi.org/10.1136/jnnp-2019-322469.

Tyszka JM, Pauli WM. In vivo delineation of subdivisions of the human amygdaloid complex in a high-resolution group template. Hum Brain Mapp 2016;37:3979–98. https://doi.org/10.1002/hbm.23289.

Figure legends

Figure 1. Amygdala segmentation and morphovolumetric analysis using the 7TAMIbrain Amygdala atlas.

A. Sagittal, coronal and axial views represent manual segmentation of a single atlas of amygdala in the 7TAMIbrain template space (a high-resolution MRI brain template constructed from thirty subjects with 3-dimensional T1-weighted magnetization-prepared 2 rapid acquisition gradient echoes (3D MP2RAGE) images acquired at 7T(Besson et al., 2016)) named 7TAMIbrain Amygdala atlas. B. Results of an automatic segmentation of amygdala of one subject using the symmetric image normalization (SyN) registration method(Avants et al., 2008), by applying the estimated deformation field on the 7TAMIbrain Amygdala atlas. C. 3D morphometric measures are directly extracted from this mask of segmentation of the left and right amygdala.

Figure 2. Epileptogenicity profiles and network organization in focal seizures with amygdala enlargement.

A. Epileptogenicity profiles across different brain regions. Normalized mean Connectivity Epileptogenicity Index (cEI (Balatskaya et al., 2020)) values (± SD) are shown for the following structures: amygdala, Amy; hippocampus, Hipp; rhinal cortex, RC; parahippocampal cortex, PHC; temporal basal cortex, TB; anterior lateral temporal cortex, TLant; posterior lateral temporal cortex, TLpost; anterior insula, INSant; posterior insula, INSpost; dorsolateral prefrontal cortex, DLPFC; orbitofrontal cortex, OFC; ventrolateral prefrontal cortex, VLPFC; dorsomedial prefrontal cortex, DMPFC; ventromedial prefrontal cortex, VMPFC; lateral premotor cortex, PML; mesial premotor cortex, PMM; primary motor cortex (including central operculum), M1; primary sensory cortex, S1; parietal operculum, OP; mesial superior parietal lobule, SPLmes; lateral superior parietal lobule, SPLlat; inferior parietal lobule, IPL; pulvinar thalami, Thal; caudate nucleus, NC.

B. Epileptogenic network types. Four distinct profiles were identified, based on the cEI: mesial temporal, TM; temporal-insular, T-INS; temporal-insular-prefrontal, T-INS-PFC; prefrontal - temporal mesial, PFC-TM. Maximal cEI values are shown for the same structures as in Fig 2A.

Figure 3. Illustrative case of focal epilepsy with amygdala enlargement and temporo-insular epileptogenic network (Patient 2).

A. Patient's 3D cortical surface rendering with implanted stereoelectroencephalographic (SEEG) electrodes. The maximal Connectivity Epileptogenicity Index (cEI) values are represented as spheres on the respective contacts according to a color map.

B. Mid rostrocaudal section through the right and left amygdala on the coronal plane of the patient's 7T T1-weighted magnetization-prepared 2 rapid acquisition gradient echoes (T1-w MP2RAGE) image. BL, basolateral nucleus; BM, basomedial nucleus; Cen, central nucleus; CMN, cortico-medial nuclear group; Cl, claustrum; La, lateral nucleus; OT, optic tract; Pu, putamen. Note a prominent extension of the left amygdala laterally (arrow), towards the neighboring claustrum and the amygdalo-striatal transition area. The morphovolumetric analysis showed a bilateral amygdala enlargement.

C. SEEG recordings of a habitual seizure that starts from the left superior temporal gyrus and rapidly involves left mesial temporal structures. Note a readily distinguishable delta-brush seizure-onset pattern followed by low-voltage fast discharge in gamma band on the external contacts of electrode T', exploring anterior aspect of T1 (L T1ant). Its posterior aspects (Heschl's gyrus, planum temporale) are affected simultaneously as a part of the EZ network, with a less sustained rapid discharge. The left temporal pole, amygdala (L Amy), rhinal cortex and anterior hippocampus are involved with a latency of 9 sec, thus belonging to the PZ network. Some left extra-temporal regions (insula, L INSpost; frontal operculum, L FOp) as well as some right T1 subregions (Heschl's gyrus, planum temporale) are subsequently involved in the PZ network.

D. Maximal cEI obtained in each recorded structure in two spontaneous seizures, demonstrating maximal epileptogenicity in the left anterior T1, followed by the ipsilateral pulvinar, Heschl's gyrus, planum temporale, anterior insula and the mesial temporal structures.

Table 1. Patient characteristics.

Patient (sex)	Age at epilepsy onset (y)	History/Context at onset of epilepsy	Subjective ictal signs	Objective ictal signs	GAD-7	NDDI-E	MRI visual analysis	Epilepsy type	Surgical procedure	Surgical outcome (Engel)	Histo-pathology
1 (f)	24	Anxiety	Unpleasant anticipatory sensation, ascending epigastric sensation, dizziness	LOC, behavioral arrest, OAA, bilateral blinking, pallor, bilateral tonic arm posture	9	15	R AE	R Temporal	ATL	III	FCD 3a
2(f)	10	Fall from a horse	Auditory illusions; sudden feeling of anxiety or intense fear, frightening presence behind her	Aphasia, LOC, behavioral arrest, fearful face expression, L head deviation, R hand dystonic posture	10	19	L AE	L Temporal	Tailored resection	II	FCD 1
3 (f)	5	FC	ascending epigastric sensation, déjà-vu, heat, palpitation	Pallor, OAA, salivation, LOC	13	15	R AE	R Temporal	ATL	I	HS
4 (f)	38	Anxiety, cannabis abuse, compulsive behavior	euphoric sensation, ascending epigastric sensation, anxiety, palpitation, thoracic pressure	Behavioral arrest, LOC, bilateral blinking, rictus, L head version	19	18	L AE	L Temporal	ATL	III	Mild gliosis
5 (f)	31	Domestic violence, PTSD	Painful/burning feeling in L arm, then L face then L hemibody	Aphasia, LOC, OAA, bilateral dystonic hand posture, L head version	12	22	R AE	R Temporal	ATL	I	HS
6 (f)	24	Depression, suicide attempts, PNES	Tingling or painful sensation L arm, L hemibody	LOC, OAA, L facial contraction, L manual automatisms	17	23	L AE	L Temporal	Tailored resection	IV	Mild gliosis

7 (m)	12	No	Dizziness, floatation feeling, auditory illusion	Behavioral arrest, LOC, OAA, verbal automatisms, facial flushing, polypnea, L head version	10	9	L AE	L Temporo-insular	Tailored resection	II	FCD1b
8 (m)	13	No	Suffocation, burning sensation in the right hemibody	R head version, hypersalivation, vocalization	7	6	L AE	L Insulo-perisylvian	TC	NA	NA
9 (m)	28	FC; Bipolar disorder	Well-being sensation, euphoria, floating sensation	LOC, verbal and gestural automatisms, laughter	4	13	R AE, AH & temporo-polar hypersignal	R Temporo-frontal	ATL, VNS, DBS	III	FCD 2b
10 (f)	42	Depression; fall into a well	Déjà-vu; cephalic electric sensation	LOC, OAA, gestural automatisms	14	19	L AE & AH	L Temporal	ATL; VNS	III	FCD 1a
11 (f)	16	Domestic violence; anxiety	No	Anxious face expression, LOC, verbal automatisms	6	14	R AE & AH	L&R fronto-temporal	VNS	NA	NA
12 (f)	4	FC; domestic violence, recurrent psychotraumatic events; depression	Painful cephalic sensation, intense fear	Fearful face expression, vocalization, psychomotor agitation, L arm dystonic posture, R gestural automatisms, R head version	10	15	R AE & AH	R Temporo-insulo-frontal & L temporal	TC	NA	NA

Abbreviations: AE, amygdala enlargement; AH, amygdala hypersignal; ATL, anterior temporal lobectomy; DBS, deep brain stimulation; FC, febrile convulsions; FCD, focal cortical dysplasia; GAD, Generalized Anxiety Disorder Scale; HS, hippocampal sclerosis; L, left; LOC, loss of consciousness; NA, non-applicable; NDDI-E, Neurological Disorders Depression Inventory-Epilepsy; OAA, oro-alimentary automatisms; PNES, psychogenic non-epileptic seizures; PTSD, post-traumatic stress disorder; R, right; TC, thermocoagulations; VNS, vagal nerve stimulation; y, years.

Table 2. Amygdala volumetric and morphometric features.

Patient (sex)	MRI visual analysis	Amygdala Volume (mm3)		Volume asymmetry (%)	Normalized volume compared to HC (z-scores)		Eccentricity (z-scores)		Elongation (z-scores)	
		Right	**Left**		**Right**	**Left**	**Right**	**Left**	**Right**	**Left**
1 (f)	R AE	1429.7	1377.4	1.9	1.6	1.4	3.5	3.8	0.3	0,2
2(f)	L AE	2010.7	2314.4	7.0	8.9	13.6	2.6	3.3	3.8	5,2
3 (f)	R AE	1927.0	1878.0	1.3	4.0	4.0	-0.8	0.0	-0.9	-0,1
4 (f)	L AE	1539.0	1529.0	0.3	2.8	3.2	-2.8	-6.4	-2.2	-4,1
5 (f)	R AE	2126.0	1805.0	8.2	6.9	4.2	-1.4	-0.5	-1.3	-0,6
6 (f)	L AE	1616.0	1657.0	1.3	4.7	5.8	0.5	0.8	0.5	0,8
7 (m)	L AE	1593.2	1661.0	2.1	0.7	1.7	3.3	2.5	-0.4	-1,0
8 (m)	L AE	1893.2	1802.3	2.5	3.1	2.7	-2.8	-0.3	-1.9	-0,4
9 (m)	R AE & AH	2117.0	1894.0	5.6	5.4	3.8	-2.5	-1.8	-2.0	-1,7
10 (f)	L AE & AH	2001.0	2331.0	7.6	5.1	9.2	2.6	2.1	3.8	2,8
11 (f)	R AE & AH	1711.5	1719.0	0.2	1.2	1.7	3.6	3.5	7.0	5,9
12 (f)	R AE & AH	1561.4	1519.8	1.4	5.9	6.0	-1.5	-2.0	-1.4	-1.8

Abbreviations: AE, amygdala enlargement; AH, amygdala increased signal; HC, healthy controls; L, left; R, right

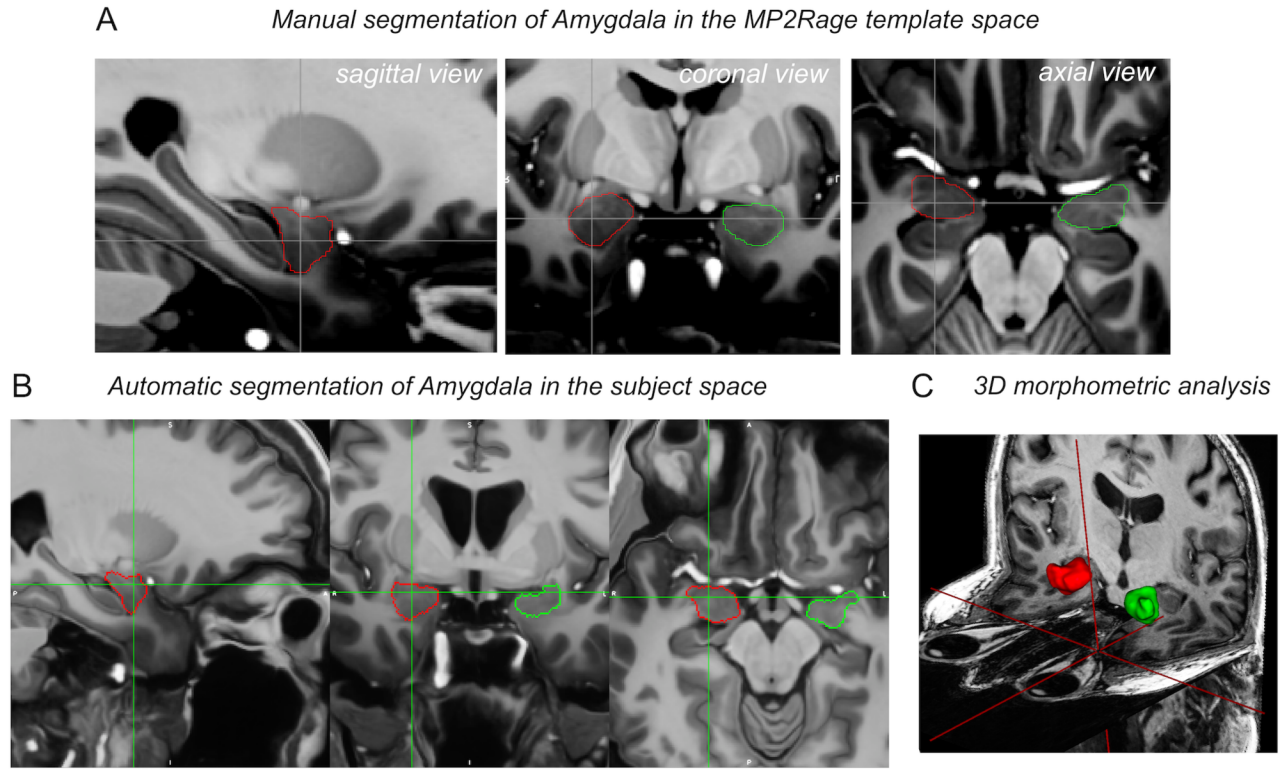
A
Manual segmentation of Amygdala in the MP2Rage template space
sagittal view
coronal view
axial view
B
Automatic segmentation of Amygdala in the subject space
C
3D morphometric analysis

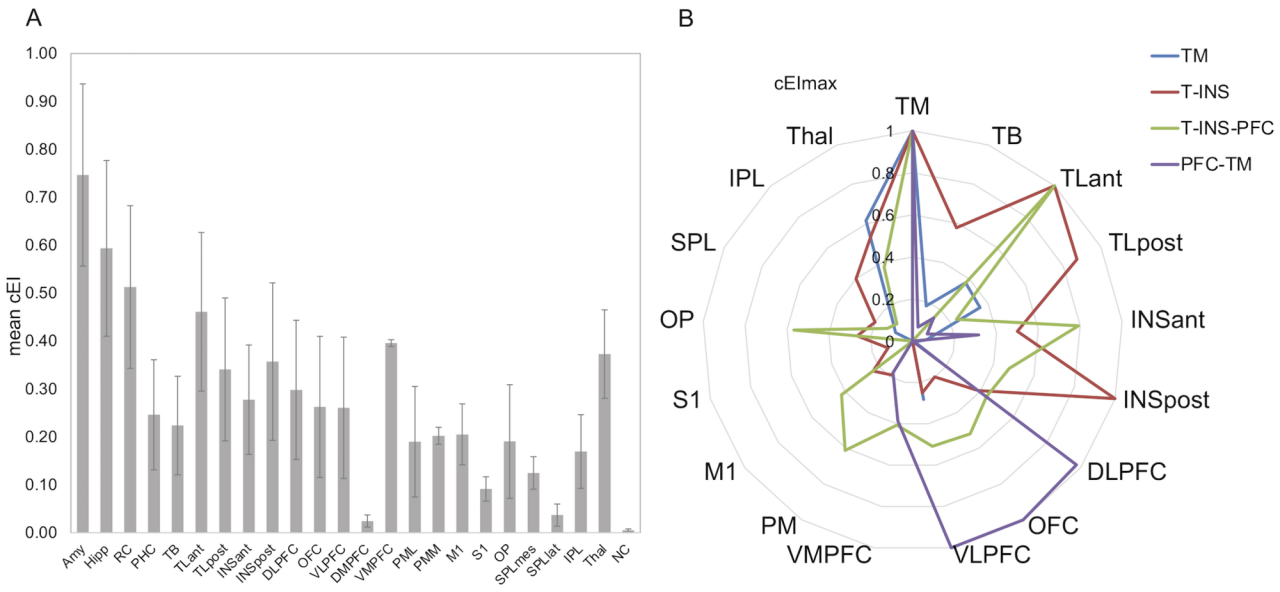
A
mean cEI
1.00
0.90
0.80
0.70
0.60
0.50
0.40
0.30
0.20
0.10
0.00
Amy
Hipp
RC
PHC
TB
TLant
TLpost
INSant
INSpost
DLPFC
OFC
VLPFC
DMPFC
VMPFC
PML
PMM
M1
S1
OP
SPLmes
SPLlat
IPL
Thal
NC
B
cEImax
TM
TB
TLant
TLpost
INSant
INSpost
DLPFC
OFC
VLPFC
VMPFC
PM
M1
S1
OP
SPL
IPL
Thal
1
0.8
0.6
0.4
0.2
0
TM
T-INS
T-INS-PFC
PFC-TM

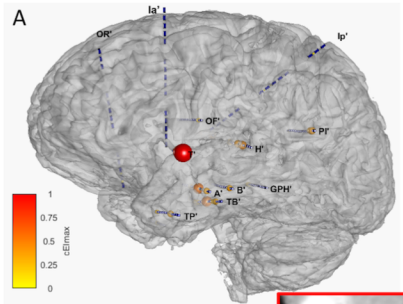
A
Ia'
OR'
Ip'
OF'
PI'
H'
A'
B'
GPH'
TB'
TP'
1
0.75
0.5
0.25
0
cElmax

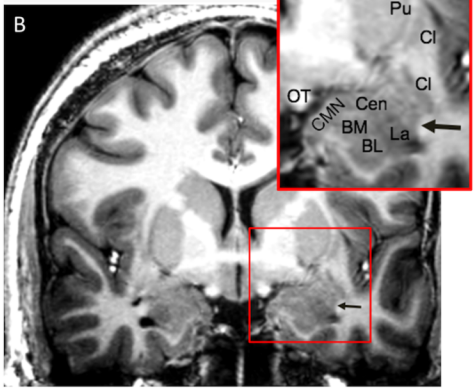
B
Pu
Cl
Cl
OT
CMN
Cen
BM
BL
La

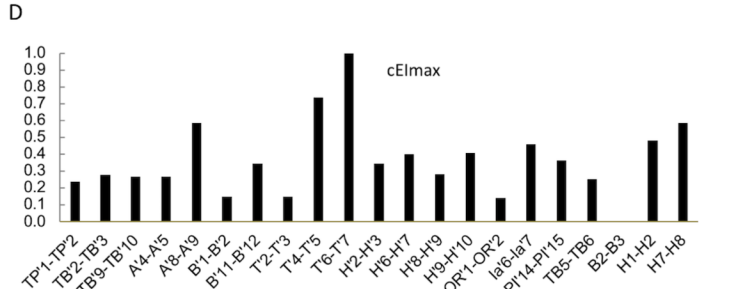
D
cElmax
1.0
0.9
0.8
0.7
0.6
0.5
0.4
0.3
0.2
0.1
0.0
TP'1-TP'2
TB'2-TB'3
TB'9-TB'10
A'4-A'5
A'8-A'9
B'1-B'2
B'11-B'12
T'2-T'3
T'4-T'5
T'6-T'7
H'2-H'3
H'6-H'7
H'8-H'9
H'9-H'10
OR'1-OR'2
Ia'6-Ia'7
PI'14-PI'15
TB'5-TB'6
B2-B3
H1-H2
H7-H8

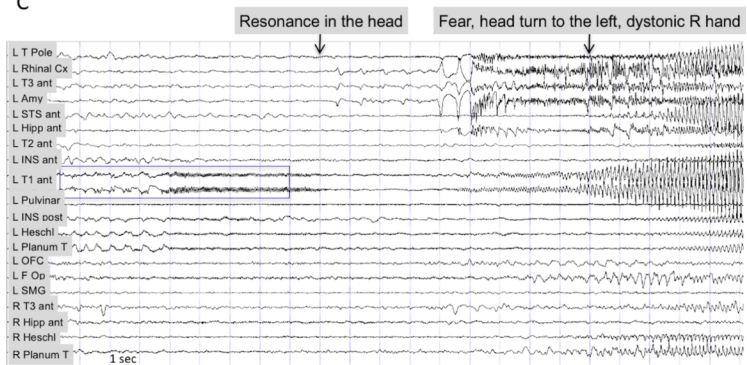
C
Resonance in the head
Fear, head turn to the left, dystonic R hand
L T Pole
L Rhinal Cx
L T3 ant
L Amy
L STS ant
L Hipp ant
L T2 ant
L INS ant
L T1 ant
L Pulvinar
L INS post
L Heschl
L Planum T
L OFC
L F Op
L SMG
R T3 ant
R Hipp ant
R Heschl
R Planum T
1 sec